THE ASTROPHYSICAL JOURNAL, 324:907–919, 1988 January 15

DENSE CORES IN DARK CLOUDS. V. CO OUTFLOW

P. C. MYERS
Harvard-Smithsonian Center for Astrophysics

AND

M. HEYER, RONALD L. SNELL, AND P. F. GOLDSMITH
Five College Radio Astronomy Observatory, and Department of Physics and Astronomy, University of Massachusetts

ABSTRACT

Sixteen dense cores in nearby dark clouds having associated low-mass stars were surveyed in the $J = 1\text{–}0$ line of ^{12}CO at 2.6 mm, and seven were found to have CO outflow. These outflows are among the weakest known, with mass loss rates of less than $10^{-8}\ M_{\odot}\ yr^{-1}$, similar to those of winds from T Tauri stars. The detection rate of outflows in cores with stars is relatively high; this indicates that outflows occur in more than half of low-mass star-core systems and that the typical outflow lasts most of the life of the star-core system. In 12 dense cores with outflows, the flow momentum is similar to or greater than the product of core mass and velocity dispersion; and the flow kinetic energy is similar to or greater than the core kinetic energy. Twelve cores with outflow have typical velocity dispersion significantly greater than that of 31 cores without outflow. These results indicate that outflows in star-core systems are sufficiently frequent; last long enough; have sufficient available momentum and kinetic energy; and have enough evidence of outflow-core interaction, in order to be the main agent of core dispersal. If so, outflows play an important role in determining the main-sequence mass of low-mass stars. Bolometric luminosities of stars within 400 pc of the Sun with CO or optical indications of outflow, or both, are typically 3–4 times greater than those without outflows. Surveys of low-luminosity stars for outflow may reveal whether this difference is due to sensitivity limitations or evolutionary changes.

Subject headings: interstellar: molecules — stars: formation — stars: pre–main-sequence

I. INTRODUCTION

In the last few years, several studies have begun to reveal the properties of condensations in nearby star-forming complexes. Molecular line observations of visually opaque regions in dark clouds in Taurus, Ophiuchus, Cygnus, and Cepheus have established the typical column density, number density, temperature, velocity dispersion, and size of "dense cores" observed in lines of ^{13}CO, $C^{18}O$, NH_3, and HC_5N (Myers, Linke, and Benson 1983; Myers and Benson 1983; Myers 1983; Benson and Myers 1983). The suggestion that such regions form low-mass stars (Churchwell, Winnewisser, and Walmsley 1978; Myers and Benson 1983) was verified by observations with the *IRAS* satellite, which found that about half of the 95 surveyed cores have associated *IRAS* point sources (Beichman *et al.* 1986). At the same time, it has become clear that many young low-mass stars have energetic outflows traced by high-velocity emission in the $J = 1\text{–}0$ ^{12}CO emission line profile (Snell, Loren, and Plambeck 1980; Edwards and Snell 1984; Lada 1985). This paper reports a survey of dense cores with embedded stars for signs of CO outflow, and an analysis of the relationship between these outflows and cores. Our main result is that outflows traced by CO are likely to be the main agent of dispersal of low-mass cores because the outflows have frequent incidence, long duration, and sufficiently great momentum and kinetic energy; and because the core line widths indicate outflow-core interaction. The observational results are presented in § II; discussed in § III; and summarized in § IV.

II. OBSERVATIONS

a) Selection

The dense cores searched for evidence of CO outflow were chosen primarily from the lists of Myers, Linke, and Benson (1983), Myers and Benson (1983), and Benson (1983). These condensations in nearby star-forming complexes, including Taurus, Ophiuchus, Cygnus, and Cepheus, are evident as opaque spots a few arcminutes in extent on the Palomar Sky Survey red prints. Most of the surveyed regions are known to have emission in the $(J, K) = (1, 1)$ line of NH_3 at 1.3 cm, which traces gas with density $10^4\ cm^{-3}$ or greater. Over half of these are further known to have embedded *IRAS* sources (Beichman *et al.* 1986), and presence of an *IRAS* source was given high priority in selecting cores to be surveyed for CO outflow.

b) Search Method

Observations were made with the 14 m diameter telescope of the Five College Radio Astronomy Observatory in New Salem, Massachusetts, primarily between 1984 May and 1985 January. Each core was first observed by position switching in the $J = 1\text{–}0$ line of CO at 2.6 mm, at each of nine positions in a 3×3 right ascension-declination grid with 2′ spacing. Spectral resolution of 100 kHz was used, and the typical rms noise in one channel was ~ 0.2 K, giving a typical signal-to-noise ratio 15 at line peak. The main beam had FWHM 45″ and forward-scattering efficiency 0.70, the latter based on observation of the Moon. The search pattern was chosen to cover the typical

FWHM extent of a core map in the NH_3 line and to reduce the chance that evidence of CO outflow would be missed because of coarse sampling. The search grid was centered on the position of peak NH_3 line emission, if no stellar source was known; or on the stellar position, from the *IRAS Point Source Catalog* or near-infrared observations (Benson, Myers, and Wright 1984). If any of the nine CO spectra showed significant asymmetry, wings, or shoulders, the map was either extended, or filled in, or both. If the map showed localized high-velocity emission around the infrared source, this was considered evidence of outflow. In addition, all outflows identified here show significant spatial separation of the red and blue line wings, indicating that the outflow is bipolar—as are most outflows (Lada 1985). Longer integration spectra were taken in both the ^{12}CO and ^{13}CO lines at the positions of maximum blue-wing and red-wing emission. The cores searched for CO outflow are listed in Table 1. The observed and deduced outflow properties are listed in Tables 2–4.

c) Results

Table 1 gives the NH_3 core name (col. [1] used by the first reference in column (2); the *IRAS* name of the associated star, if any (col. [3]); other references to the star (col. [4]); the coordinates of the center of the mapping grid (cols. [5] and [6]); line parameters of the average of the nine map-grid spectra (cols. [7]–[9]); CO outflow status deduced from the maps and spectra (col [10]); and miscellaneous notes (see footnotes). The table is divided into three parts according to the distance r between the peak of the NH_3 core map and the nearest associated star. The star-core distance is expressed in terms of the core diameter R, defined as the geometric mean of the maximum and minimum FWHM diameters of the NH_3 (1, 1) line intensity map. The star is considered associated if it satisfies the *IRAS* criteria in Beichman *et al.* (1986): *IRAS* detection at either 25 μm, or at both 60 and 100 μm. Then Table 1 lists cores having (a) the nearest associated star within

TABLE 1

^{12}CO $J = 1 \rightarrow 0$ LINE EMISSION FROM LOW-MASS DENSE CORES

CORE (1)	REFERENCE (2)	STAR (3)	REFERENCE (4)	(0, 0) POSITION R.A. (1950) (5)	(0, 0) POSITION Decl. (1950) (6)	T_R (K) (7)	V_{LSR} (km s^{-1}) (8)	ΔV (km s^{-1}) (9)	CO Outflow (10)
				Star-Core Distance = 0–1 Core Diameters					
L1489	1, 2, 3, 4	04016+2610	4–6	$04^h01^m40\overset{s}{.}6$	26°10′48″	5.9	7.0	1.8	Y
L1524	7	04263+2426[a]	6	04 26 21.6	24 26 26	6.9	6.3	3.1	N
L1535	8	04325+2402	9	04 32 31.6	24 02 07	7.4	6.3	2.0	Y[b]
HCL 2A	10	04365+2535	6	04 36 31.2	25 35 56	6.8	6.1	2.5	N
L1527	7	04368+2557	9	04 36 49.3	25 57 16	6.5	6.4	3.2	N
TMC 1	1, 2, 11	04381+2540	5	04 38 07.6	25 40 48	5.3	6.4	3.2	N
B35	2	05417+0907	5	05 41 42.0	09 07 00	7.8	11.7	2.3	Y
L43	1, 2	16316−1540	5, 6, 12	16 31 38.0	−15 40 50	8.5	0.2	1.8	Y[c]
L778	2	19244+2352	5	19 24 26.4	23 52 37	4.9	11.0	3.7	Y
L1152	1, 2	20353+6742	5, 6	20 35 20.5	67 42 36	5.0	3.0	2.1	N
L1082A	7	20520+6003	5	20 52 05.1	60 03 20	3.4	−2.7	3.1	N
L1174	1, 2	20597+6800	5	20 59 46.3	68 01 04	7.6	2.4	3.6	N
L1172D	1, 2	21017+6742	5	21 01 44.9	67 42 32	7.4	2.9	3.2	Y
L1031B	1, 2	21454+4718	5, 13	21 45 27.9	47 18 12	6.8	3.8	3.7	Y[d]
L1262	1, 2, 4	23238+7401	5	23 23 47.9	74 01 03	7.4	4.0	2.3	N
				Star-Core Distance = 1–3 Core Diameters					
L1495	1, 2	04112+2803[e]	5, 6	04 10 57.5	28 03 53	8.4	6.4	2.6	N
B217	1, 2	04248+2612	5, 6	04 24 59.7	26 12 41	4.5	7.1	2.2	N
TMC 2A	1, 2, 3	04288+2417	6	04 28 49.2	24 17 58	7.6	6.1	2.6	N
		04292+2422	5, 6	04 29 13.1	24 43 21	5.4	5.9	3.0	N
L1536	1, 2, 4	04303+2240	4–6	04 30 19.3	22 40 22	4.0	5.9	2.4	N
TMC 1C	1, 2, 10, 14	04380+2553	9	04 37 02.3	25 53 51	5.1	5.9	2.8	N
		04385+2550	5, 6	04 38 34.6	25 50 44	4.1	5.8	2.5	N
L234A	1, 2	16451−1045	9	16 45 21.0	−10 46 33	10.4	3.1	1.0	N
				No Associated Star					
L1517	1, 2	...	...	04 52 07.2	30 33 18	6.6	5.9	1.2	N
L1582	2, 4[f]	...	...	05 29 14.2	12 28 59	13.3	10.1	1.7	N
L234E	1, 2	...	...	16 45 18.0	−10 51 43	8.5	3.1	1.1	N
L63	1, 2	...	...	16 47 21.0	−18 01 00	7.4	5.8	1.2	N

[a] 04263+2426 = Haro 6–10, the exciting source of a Herbig-Haro object (Elias 1978*b*).
[b] CO outflow maps and spectra presented in Heyer *et al.* 1987.
[c] CO outflow also found by Levreault (1985).
[d] CO outflow also found by Levreault (1983).
[e] 04112+2803 lies ~1′ SE of CW Tau, which has no closer *IRAS* counterpart.
[f] The near infrared source found in ref. (4) was not found by *IRAS* and is therefore not counted as associated.

REFERENCES.—(1) Myers and Benson 1983; (2) Benson 1983; (3) Gaida, Ungerechts, and Winnewisser 1984; (4) Benson, Myers, and Wright 1984; (5) Beichman *et al.* 1986; (6) Myers *et al.* 1986; (7) Benson, Goodman, and Myers 1988; (8) Ungerechts, Walmsley, and Winnewisser 1982; (9) *IRAS Point Source Catalog*; (10) Cernicharo, Guelin, and Askne 1984; (11) Little *et al.* 1979; (12) Herbst and Warner 1981; (13) Elias 1978*a*; (14) Benson and Myers 1983.

TABLE 2

CO OUTFLOW VELOCITIES AND POSITIONS OF PEAK WING MAP EMISSION

	BLUE WING				RED WING			
CORE	V_{min}[a]	V_{max}[a]	$\Delta\alpha$	$\Delta\delta$	V_{min}[a]	V_{max}[a]	$\Delta\alpha$	$\Delta\delta$
L1489	4.0	6.0	0.′0	0.′0	7.5	9.5	−2.′0	0.′0
B35	6.0	10.5	1.0	1.0	13.5	18.5	2.0	1.0
L43	−4.5	−0.5	−0.5	−1.0	1.0	5.0	0.0	2.5
L778	1.5	8.5	1.0	2.0	13.5	20.5	−2.0	−2.0
L1172	−5.0	1.0	1.0	−1.0	4.0	10.0	0.0	0.0

[a] In km s^{-1}.

NOTE.—V_{min} and V_{max} are the LSR velocity limits used in integrating the spectral wing emission to produce the CO maps in Figs 1*a*–5*a*. For each blue wing, V_{min} is approximately the smallest LSR velocity at which emission was detected and V_{max} is the limit chosen so as to give good spatial separation of the red and blue maps and good signal-to-noise ratio in each map. For each red wing, V_{min} is the limit chosen as for V_{max} in the blue wing, above, and V_{max} is approximately the largest LSR velocity at which emission was detected.

TABLE 3

OUTFLOW ENERGETICS

Core	M ($M_\odot$)	P ($M_\odot$ km s^{-1})	E (10^{43} ergs)	R (pc)	$\langle v\rangle$ (km s^{-1})
L1489	0.04	0.04	0.12	0.1	1.0
B35	0.86	2.0	6.4	0.4	2.4
L43	0.11	0.12	0.52	0.2	1.2
L778	0.08	0.28	2.1	0.3	3.5
L1172	0.88	2.3	14	0.5	2.6

NOTE.—All quantities are calculated as in Goldsmith *et al.* 1984. Outflow mass M, momentum P, and kinetic energy E are sums over red- and blue-shifted maps. Size R and mean velocity $\langle v\rangle$ are averages over red- and blue-shifted maps. Adopted distances are given in Table 5.

one core diameter of the core peak; (*b*) the nearest associated star within one to three diameters; and (*c*) no associated star.

Table 1 shows our main result: stars in cores are much more likely to have CO outflow than are stars near cores or cores without stars. Seven of 16 cores with $r/R < 1$ have CO outflow, while none of six cores with $1 \leq r/R \leq 3$, and none of four cores with no associated star, has an outflow. Each outflow in L1489, B35, L43, L778, and L1172 is displayed in Figures 1–5, in two ways: (*a*) a map of the red and blue CO line wings, next to a map, to the same scale, of NH_3 line emission; and (*b*) ^{12}CO and ^{13}CO spectra at the positions of maximum red- and maximum blue-wing emission. Two outflow sources in our survey are listed in Table 1 but not shown in map form because they were first reported elsewhere: 04325+2402 in L1535 (Heyer *et al.* 1987) and 21454+4718 in L1031 (Levreault 1983). The velocity limits of the line wing integration, and the positions where the red and blue wing maps are maxima, are given in Table 2. Further information about each outflow is given in Table 3 (energetics: outflow mass, momentum energy, spatial extent, and velocity extent), and Table 4 (dynamics: dynamical time, outflow force, mechanical luminosity, and mass loss rate). In Tables 3 and 4, each quantity is defined as in Goldsmith *et al.* (1984), with no correction for high excitation temperature, high optical depth, or outflow orientation. The effect of these corrections is discussed in § III*b*). The following paragraphs describe each source individually, and then source properties common to the group.

L1489 (04016+2610).—L1489 is at the western edge of the Taurus complex (distance 140 pc) and is visible on the POSS red print in both absorption and faint reflection. The star 04016+2610 is optically invisible and is located at the western edge of the NH_3 core. The CO outflow is one of the smallest and weakest known, with extent ~0.1 pc, energy 1×10^{42} ergs, and mass loss rate 2×10^{-9} $M_\odot$ yr^{-1}. The maps of the high-velocity emission have significant overlap with each other and with the NH_3 map. The NH_3 core is not centered between the wing maps as it is in the well-known outflow sources in L1551 and B335. The ^{12}CO spectra do not have the usual extensive wings indicative of outflow, merely a slight "shoulder," and shift in their centroid velocities. Because of this lack of "wings" one may question whether the observed motions are actually due to outflow or rotation. But rotation is unlikely because the point mass needed to account for the observed values of R and $\langle v\rangle$ in Table 3 is $23/\sin^2 i$ $M_\odot$, where i is the inclination between the rotation axis and the line of sight. This mass is significantly greater than the probable mass of 04016+2610—about 1 $M_\odot$, as is typical of stars in the Taurus complex (Cohen and Kuhi 1979). It is also much greater than the mass of gas within the lowest contour of NH_3 emission in Figure 1*a*, 4 $M_\odot$, based on the density estimate of Myers and Benson (1983). Furthermore, the lines of ^{13}CO and NH_3 show no systematic shift in velocity with position, as would be expected for simple rotation.

B35(05417+0907).—B35 is part of the ring of bright-rim dark clouds surrounding λ Ori (distance 500 pc). Its CO and far-infrared emission were studied by Lada and Black (1976) and Lada *et al.* (1981). The NH_3 core and associated star discussed here are in a visually opaque portion of the cloud ~2′ SW of the CO peak and ~2′ E of the T Tauri star V630 Ori. The star is optically invisible and lies near the peak of the NH_3 emission. The CO line wing maps are each elongated along the line joining their positions of peak emission, and the maps have considerable overlap. Neither the star nor the NH_3 map peak lies between the wing map peaks. The ^{12}CO spectra have pronounced wings. The outflow is one of the most energetic in the group discussed here, and it has the largest mass loss rate:

TABLE 4

OUTFLOW DYNAMICAL PROPERTIES

Core	τ (10^4 yr)	F (10^{-5} $M_\odot$ km s^{-1} yr^{-1})	L (10^{-4} $L_\odot$)	$\dot{M}_*$ (10^{-8} $M_\odot$ yr^{-1})
L1489	13	0.02	4	0.2
B35	18	1.1	29	11
L43	17	0.05	2	0.5
L778	8	0.19	11	1.9
L1172	17	0.66	36	6.6

NOTE.—All quantities are calculated as in Goldsmith *et al.* 1984. Dynamical time τ, force F, mechanical luminosity L, and stellar mass loss rate $\dot{M}_*$ are averages over the red- and blueshifted maps. Adopted distances are given in Table 5.

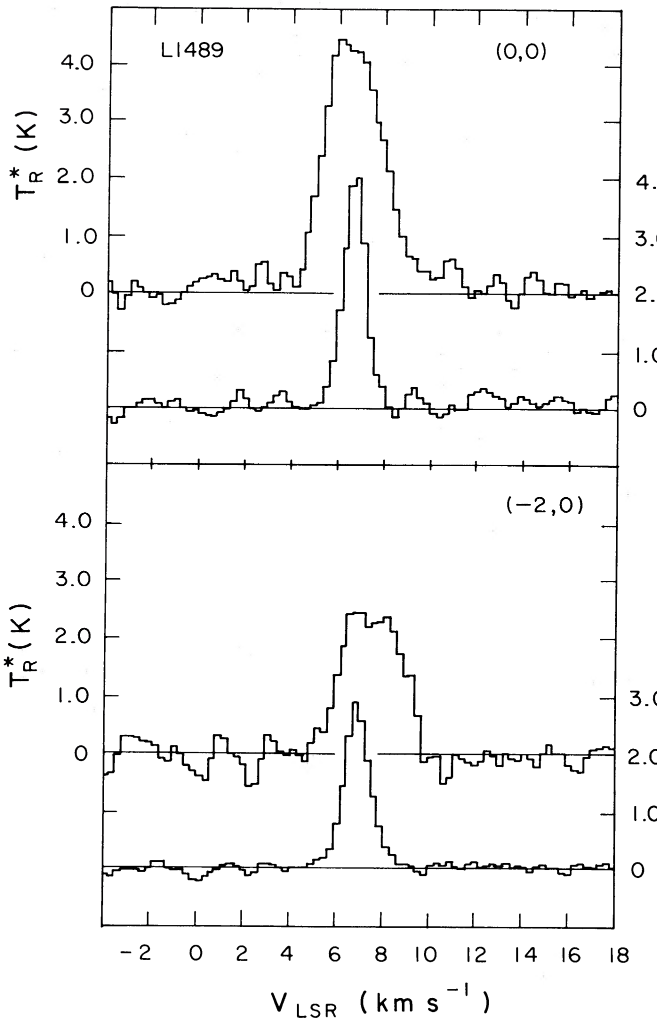

FIG. 1a

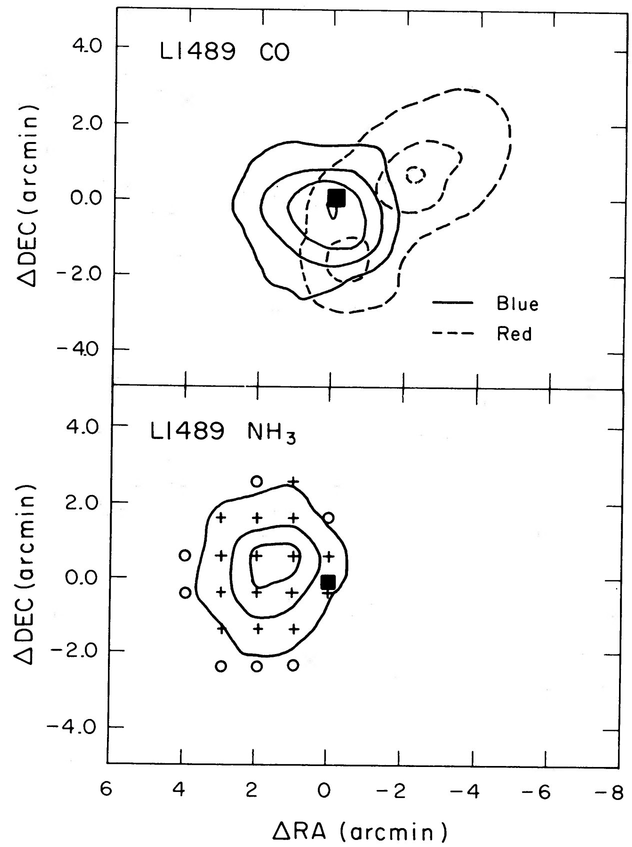

FIG. 1b

FIG. 1.—L1489. (*a*) Contour maps of ^{12}CO $J = 1$–0 line wing intensity T_R integrated over the velocity ranges in Table 2; and of NH$_3$ $(J, K) = (1, 1)$ line intensity T_A^*, from Benson (1983). The (0, 0) position is given in Table 1; each filled square marks the associated *IRAS* source in Table 1. CO contours: lowest level, 1 K km s^{-1}; increment, 1 K km s^{-1}. NH$_3$ contours: lowest level, 0.1 K; increment, 0.3 K. (*b*) $J = 1$–0 spectra of ^{12}CO and ^{13}CO emission at positions of maximum blue-wing (*top*) and maximum red-wing (*bottom*) integrated intensity, given in Table 2.

1×10^{-7} $M_\odot$ yr^{-1}, similar to that of B335 (Goldsmith *et al.* 1984).

L43(*16316−1540*).—L43 lies in the northern part of the Ophiuchus complex (distance 160 pc). It contains the reflection nebulae RNO 90 and 91 (Cohen 1980) separated by $\sim 8'$ and illuminated by T Tauri stars (Herbst and Warner 1981). The NH$_3$ core, the star 16316+1540, and the CO outflow discussed here are associated with RNO 91; the CO outflow (blue wing only) was also discovered by Levreault (1985). The star is optically visible, lies at the western edge of the NH$_3$ core, and is approximately centered between the outflow wing maps. The wing maps are well separated and elongated approximately along the line joining their peaks. The NH$_3$ core does not lie between the wing maps. The outflow is by most measures nearly as weak as that in L1489, and its mechanical luminosity is the smallest in the group: 2×10^{-4} $L_\odot$. The ^{12}CO spectra have distinct shoulders.

L778(*19244+2352*).—L778 is a filamentary dark cloud in Vulpecula with a diffuse tail and an opaque arc-shaped head, which contains the NH$_3$ core discussed here. Its distance is uncertain; we adopt 250 pc as in Beichman *et al.* (1986). The *IRAS* source 19244+2352 is well centered in the core, although two other *IRAS* sources (19243+2351 and 19245+2347) have similar spectra and lie near the core edge, a few arcminutes away. The CO wing maps are complex, with two distinct blue lobes and one red lobe. The northern blue lobe is aligned with the NH$_3$ core, the star 19244+2352, and the red lobe, while the southern blue lobe has no obvious counterparts in a simple bipolar pattern. The size and energy of the outflow are intermediate among the five considered here. The ^{12}CO line profile is the most complex of the group, with prominent self-absorption and wings.

L1172 (*21017+6742*).—L1172 is a prominent dark cloud in Northern Cepheus that contains NGC 7023, a reflection nebula surrounding the Be star HD 200775 (Mendoza 1958; distance 440 pc). An apparently unrelated outflow associated with HD 200775 was reported by Choe (1985). L1172 was mapped in ^{12}CO $J = 1$–0 line emission by Elmegreen and Elmegreen (1978). The NH$_3$ core and *IRAS* star 21017+6742 are located in visually opaque obscuration 15′ south of the

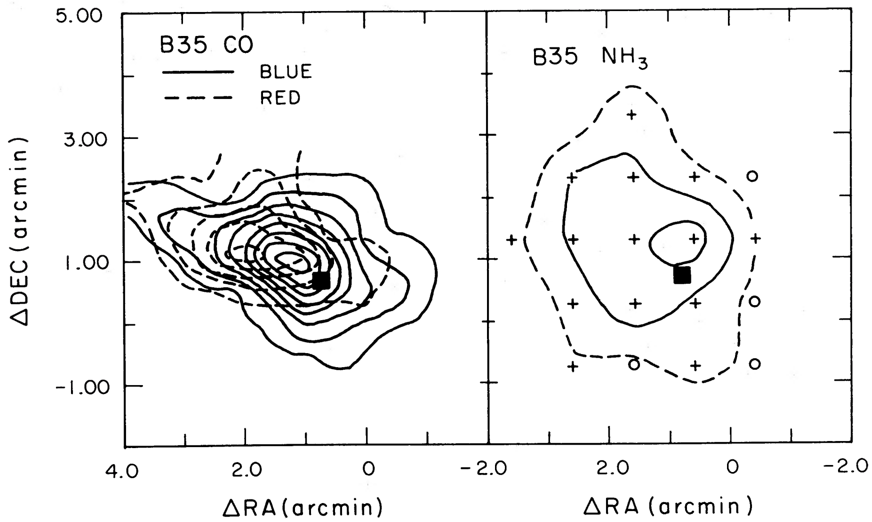

FIG. 2a

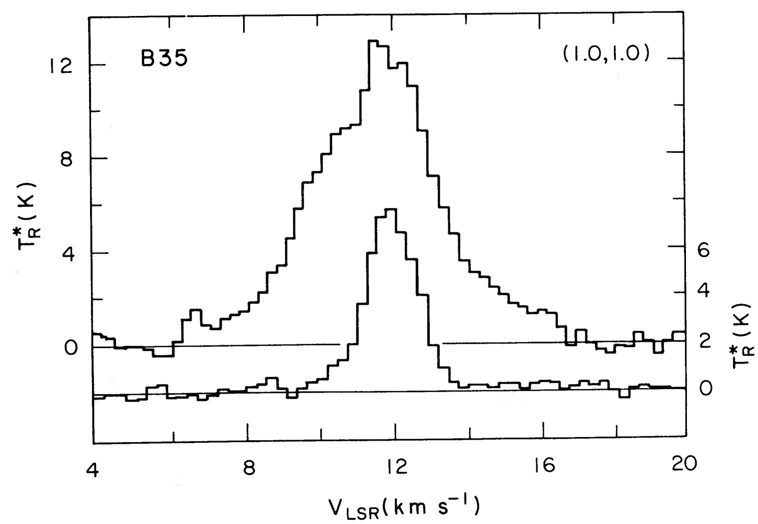

FIG. 2b

FIG. 2.—B35. Contour maps and spectra with same format as Fig. 1. CO Contours: lowest level, 1 K km s^{-1}; increment, 1 K km s^{-1}. NH_3 contours: lowest level, 0.1 K; increment, 0.1 K. The positions of maximum blue- and red-wing emission nearly coincide, so only one pair of spectra is shown.

reflection nebula. The star is optically invisible and centered in the NH_3 map. The CO wing maps are well separated, and the star and core lie between the wing maps. However, the outflow departs from the classic pattern of L1551 or B335 in that each wing map is elongated along a line approximately perpendicular, rather than parallel, to the line joining the map peaks. The outflow is the largest (0.5 pc) and most energetic (1.4×10^{44} ergs, similar to L1551 and B335) of the five discussed here. The ^{12}CO line profiles are slightly self-reversed but, as in L1489, they have no prominent wings. Also as in L1489, the point mass required to account for the line profiles by simple rotation is too large ($790/\sin^2 i\, M_\odot$) to be consistent with either the *IRAS* source or the dense core.

As a group the outflow sources studied here differ from other outflow sources in two ways: they are remarkably weak and their ^{13}CO emission is remarkably strong compared to their ^{12}CO emission. The dark cloud CO outflows of Goldsmith *et al.* (1984) were among the weakest known when they were discovered. But the source with the greatest kinetic energy in Table 3 (L1172: 1×10^{44} ergs) has kinetic energy about equal to that of the weakest source of Goldsmith *et al.* (B335). The source with median kinetic energy in Table 3 (L778: 1.4×10^{43} ergs) is weaker by a factor of 15 than the corresponding mean source of Goldsmith *et al.*, and the source with the least kinetic energy (L1489: 1.2×10^{42} ergs) is similar to HL Tau, the weakest CO outflow known (Calvet, Cantó, and Rodríguez 1983). Similarly, the greatest mass loss rate in Table 4 (B35: $1 \times 10^{-7}\, M_\odot\, yr^{-1}$ is similar to the weakest of Goldsmith *et al.* (B335). The median source (L778: $1.5 \times 10^{-8}\, M_\odot\, yr^{-1}$) is ~ 50 times weaker than that of Goldsmith *et al.*, and the weakest source (L1489: $2 \times 10^{-9}\, M_\odot\, yr^{-1}$) has mass loss rate similar to that of winds from weak T Tauri stars.

The five outflow sources are also unusual in that their peak ^{13}CO intensities $T_R(^{13}CO)$ are in many cases nearly equal to the corresponding ^{12}CO intensities $T_R(^{12}CO)$ whereas ordinarily $T_R(^{13}CO)/T_R(^{12}CO) \lesssim 0.5$. Four of the five sources have

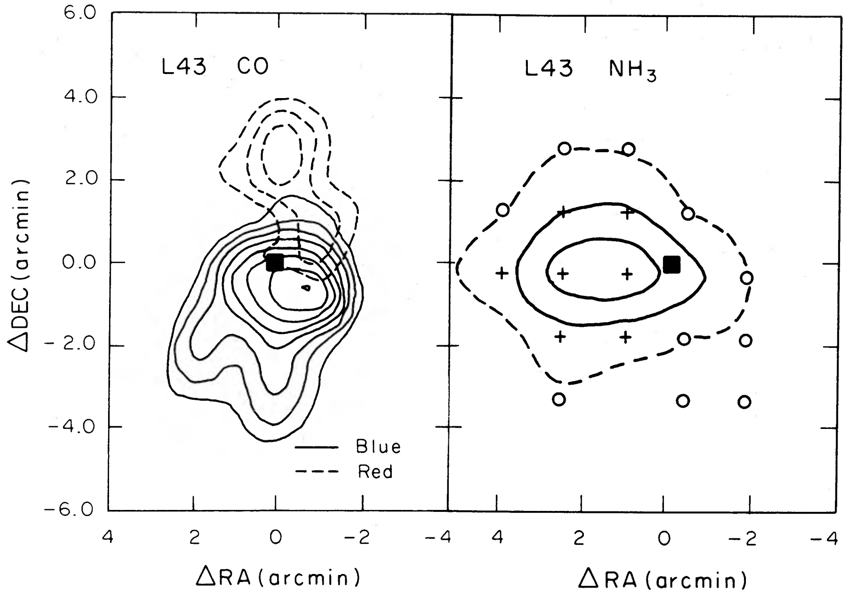

FIG. 3*a*

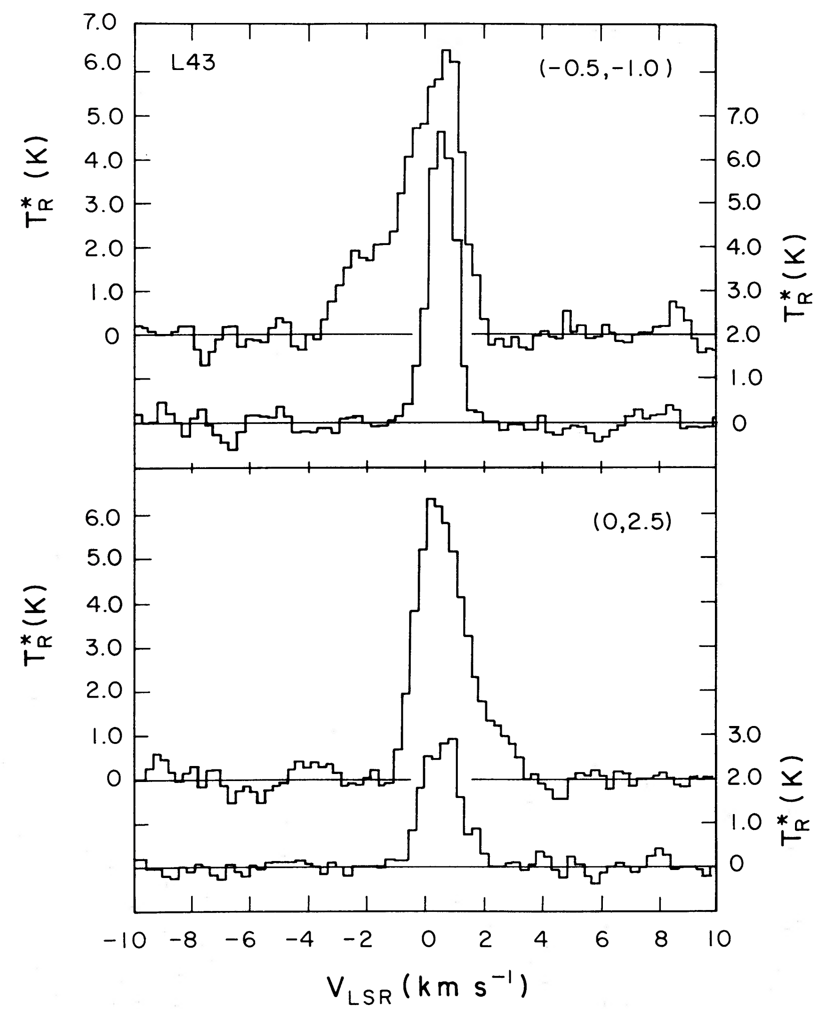

FIG. 3*b*

FIG. 3.—L43. Contour maps and spectra with same format as Fig. 1. CO contours: lowest level, 3 K km s^{-1}; increment, 1 K km s^{-1}; NH_3 contours: lowest level, 0.1 K; increment, 0.2 K.

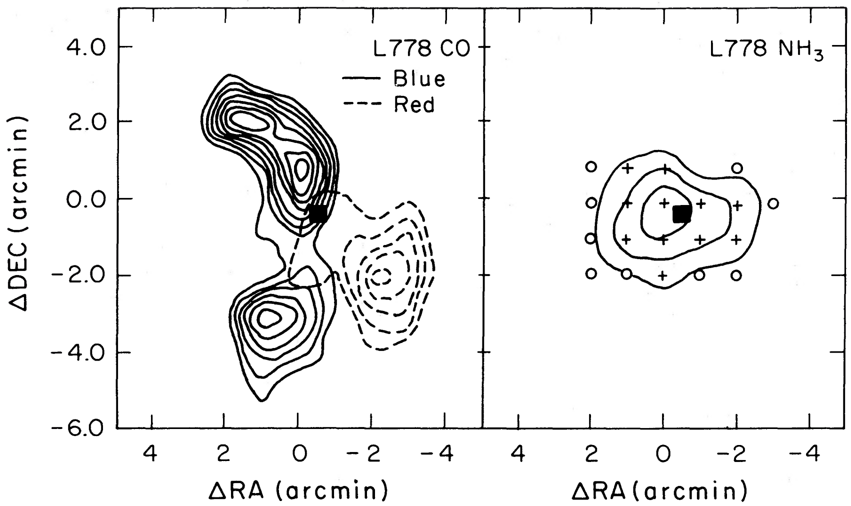

FIG. 4*a*

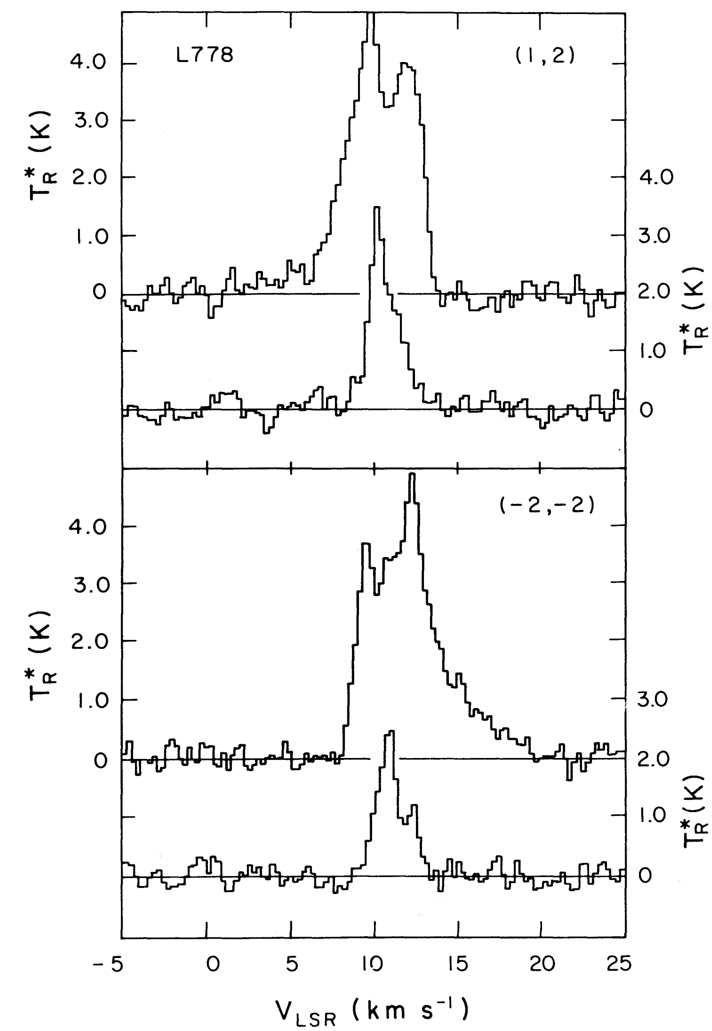

FIG. 4*b*

FIG. 4.—L778. Contour maps and spectra with same format as Fig. 1. CO contours: lowest level, 1 K km s^{-1}; increment, 0.5 K km s^{-1}. NH_3 contours: lowest level, 0.1 K; increment, 0.1 K.

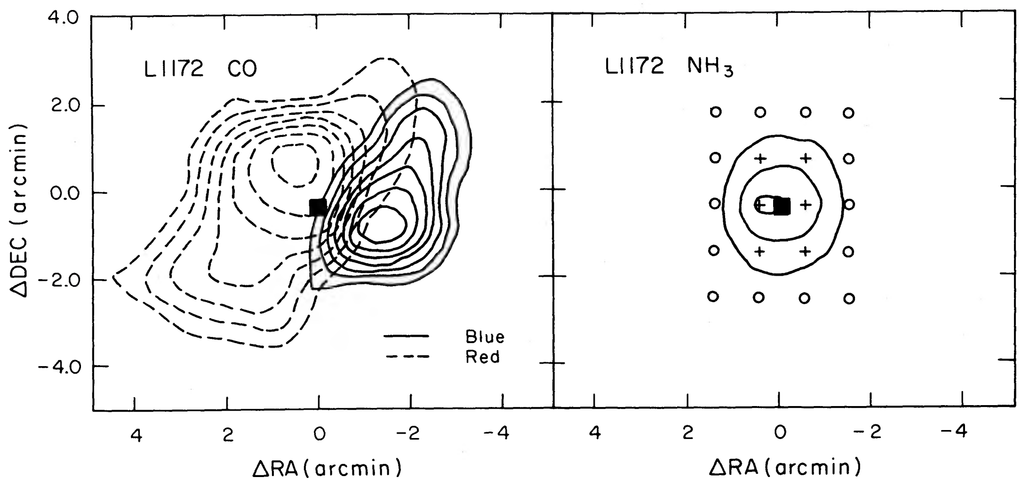

FIG. 5*a*

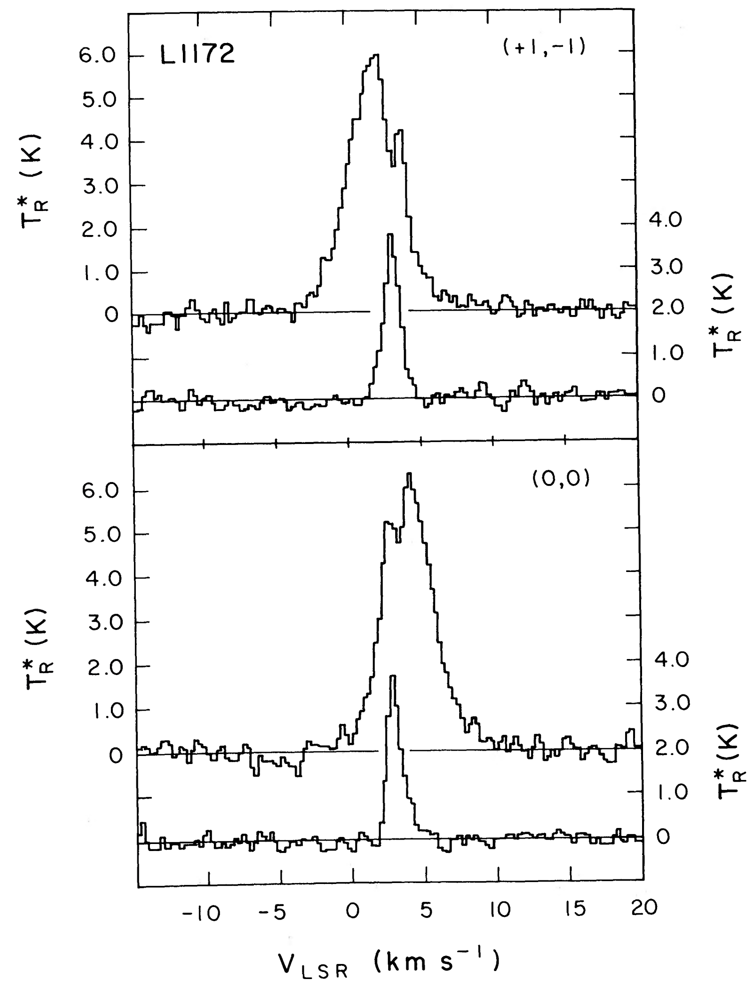

FIG. 5*b*

FIG. 5.—L1172. Contour maps and spectra with same format as Fig. 1. CO contours: lowest level, 3 K km s^{-1}; increment, 1 K km s^{-1}. NH_3 contours: lowest level, 0.15 K; increment, 0.15 K.

$T_R(^{12}CO) \approx T_R(^{13}CO)$ at the velocity of peak ^{13}CO emission in at least one map position. In contrast, only two of the 20 sources presented by Levreault (1985) have $T_R(^{12}CO) \approx T_R(^{13}CO)$ and one of these is for 16316−1540 (L43, RNO 91), a star common to both samples. This property is evident both for sources with line profiles of simple shape, as in L1489, and for sources with a self-reversed ^{12}CO profile, such as L1172D, at offset position (−1, 1). In this latter case the ^{12}CO self-absorption minimum occurs at the velocity of the ^{13}CO maximum, and the ^{12}CO and ^{13}CO line intensities at this velocity are essentially equal. This property of equal ^{12}CO and ^{13}CO intensities can be understood if the ^{13}CO line is optically thick at its peak with excitation temperature equal to that of the (also thick) ^{12}CO line. The relatively frequent occurrence of such high ^{13}CO line optical depth in the present sample may arise from the relatively high column density $A_V \gtrsim 10$ mag, which was a selection criterion of the dense cores (Myers, Linke, and Benson 1983). If so, such equal ^{12}CO and ^{13}CO line intensities may be a useful indicator of dense core gas.

III. DISCUSSION

a) Detection Rates

The detection of seven CO outflows in 16 cores with stars constitutes a remarkably high detection rate, much higher than that of outflows from stars near, but not in cores (0/8), or than that of outflows from cores without stars (0/4). It is also higher than detection rates from other surveys of low-luminosity objects ($L \lesssim 100\ L_\odot$) for CO outflows: three of 180 opaque dark clouds (Frerking and Langer 1982); three of 28 T Tauri stars (Edwards and Snell 1982); seven of 52 Herbig-Haro objects (Edwards and Snell 1983, 1984); and 21 of 71 optically selected young stars (Levreault 1985). To our knowledge only one survey has yielded a detection rate greater than 0.4, 32 of 45 (Bally and Lada 1983), and most of the sources surveyed by Bally and Lada were suspected to be outflows before their survey, and are much more luminous than in this work. The detection rates in the various surveys summarized here are not strictly comparable to each other, or to that reported here, because of differences in sensitivity, angular and spectral resolution, and in the number of points surveyed around each star. However, the detection rate reported here is high by any reasonable standard.

Three considerations suggest that the true fraction of outflows from cores with stars is still greater than 0.4, and perhaps greater than 0.7. First, six cores with NH_3 emission and with associated stars in dark clouds closer than Orion are known from previous work to have CO outflow: L1551 (Snell, Loren, and Plambeck 1980); B335, L723 and L1455 (Frerking and Langer 1982; Goldsmith *et al.* 1984); Serpens (Bally and Lada 1983) and B5 (Goldsmith, Langer, and Wilson 1986), but no NH_3 core without a star has been reported to have CO outflow. Second, any survey will miss those well-collimated bipolar outflows whose axes lie sufficiently close to 90 degrees from the line of sight, in which case the line wings will be undetectable. Third, a CO survey of the objects in this paper, with angular resolution 8 times finer than reported here, found definite outflow in one source (L1262) and probable outflow in six others, which were negative according to this paper (Terebey, Vogel, and Myers 1988). Therefore, the true rate of outflows in cores with stars is probably greater than 0.5–0.7. This high detection rate is similar to the detection of NH_3 emission in 26 cores around 34 stars known to have CO outflow (Torrelles *et al.* 1986).

These high detection rates imply that more than half of the stars in cores have outflows and that such outflows typically last for more than half of the lifetime of the star-core system. More precisely, suppose that a core with a star is detectable by NH_3 and *IRAS* observations for τ, i.e., from the time the stellar luminosity exceeds 0.1 $L_\odot$ to the time the core gas is too dispersed to be detected in NH_3 (1, 1) line. Suppose that a fraction f of such cores have detectable CO outflow sometime during their lifetime, while $1-f$ of such cores never have detectable CO outflow. Let the duration of the CO outflow be τg, $g \leq 1$. Then the likelihood h of detecting CO outflow in a star-core system is $h = fg$. Since f cannot exceed unity, it follows that $g \geq h$; and since g cannot exceed unity, it follows that $f \geq h$. We take $h = 0.5$, based on the detection rate 0.4 reported here and the reasons given earlier why this estimate is probably low. Then most cores with stars, i.e., half or more than half, have CO outflows during their detectable lifetime, and this outflow itself is detectable for most of the star-core lifetime. These relatively high values of outflow incidence and duration in star-core systems are consistent with the idea that outflows are the main agent of core dispersal.

b) Energetics

As noted in § II, the momenta, energies, and mass-loss rates of the outflows considered here are among the lowest known, and are comparable to those of winds from T Tauri stars. Despite their weakness, these outflows appear capable of supplying the momentum and energy needed to disperse their parent cores. We examine this point for 12 outflows associated with dense cores in dark clouds, by comparing P_{flow}, the component of flow momentum in the line-of-sight direction, with P_{core}, the product of core mass and one-dimensional velocity dispersion deduced from the NH_3 line maps and spectra (Myers and Benson 1983; Benson 1983). The core mass included within the FWHM contour of the NH_3 line intensity map was computed from the map dimensions and mean density. The velocity dispersion σ of the particle of mean mass ($2.3m_H$) was computed from the NH_3 line FWHM Δv according to

$$\sigma^2 = \frac{(\Delta v)^2}{8 \ln 2} + \frac{kT}{m_H}\left(\frac{1}{2.3} - \frac{1}{17}\right), \quad (1)$$

where k is Boltzmann's constant and T is the kinetic temperature, assumed to be 10 K.

The values of momentum in Table 5 span more than two decades, from $P_{core} = 0.028\ M_\odot$ km s^{-1} for L1489 to $P_{flow} = 5.3\ M_\odot$ km s^{-1} for L1551. In nearly all cases $P_{flow} \gtrsim P_{core}$, and in seven cases the ratio P_{flow}/P_{core} lies in the range 1–2. The median value of P_{flow}/P_{core} is 1.4. These relationships are shown in Figure 6, a plot of log P_{flow} versus log P_{core}. For reference, error bars corresponding to estimated random uncertainty of a factor of 2 are shown; but two systematic sources of uncertainty are probably more important. First, the core mass was evaluated within the half-maximum contour of the NH_3 (1, 1) line intensity map, but the exact contour that is appropriate to the observed line width and deduced density is uncertain and might extend twice as far as the chosen contour. If so, P_{core} would increase by a factor of 8. Second, the values of P_{flow} in Tables 3 and 5 are not corrected for three effects that, if present, tend to increase P_{flow}: (1) ^{12}CO excitation temperature greater than ambient cloud temperature (here assumed to be 10 K); (2) line wing optical depth greater than unity; and (3)

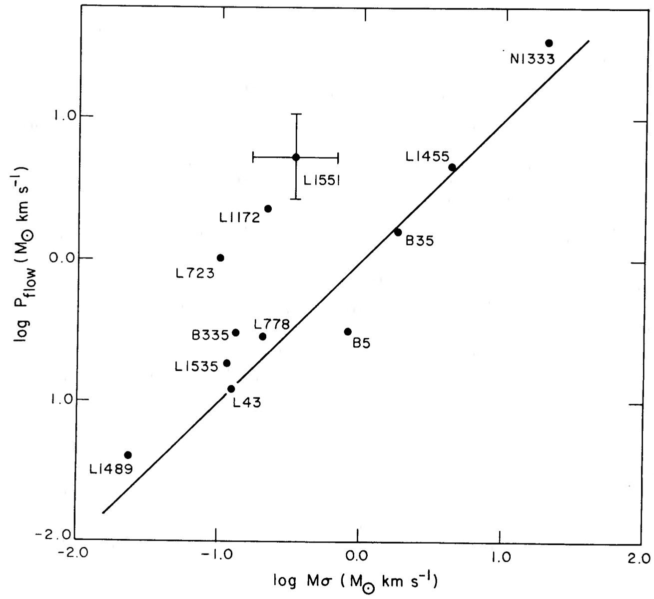

FIG. 6.—Log-log plot of outflow momentum P_{flow} vs. product of core mass M and velocity dispersion σ, for 12 cores with NH_3 maps and CO outflow listed in Table 5. Error bars indicate estimated random uncertainty of a factor of 2. Solid line indicates $P_{flow} = M\sigma$.

orientation of the flow out of the plane of the sky. Altogether, these tend to increase P_{flow} by a typical factor of ~ 5 (Goldsmith *et al.* 1984). Third, each "momentum" considered here is one dimensional and should be corrected to account for the full three-dimensional interaction if the outflow and core geometries were known better. We summarize this situation by saying the typical outflow source in a low-mass core probably has $P_{flow}/P_{core} = 1$–2, with uncertainty of a factor of 4. Since the characteristic flow velocity exceed the corresponding core velocity by a factor of ~ 10, this estimate of P_{flow}/P_{core} also implies that the ratio of kinetic energies K_{flow}/K_{core} typically exceeds unity by one order of magnitude.

These comparisons indicate that the typical outflow in a low-mass core has enough momentum and kinetic energy to substantially increase the momentum and kinetic energy of the dense core gas. Indeed, the high degree of correlation between P_{flow} and P_{core} suggests that outflow-core interaction may be the dominant source of nonthermal core motions in our sample; and that these motions "adjust" fairly sensitively to the outflow momentum. The core gas is generally close to virial equilibrium (Myers and Benson 1983), so the flow-core interaction may be able to unbind a substantial fraction of the core gas and disperse it. These momentum and energy considerations are necessary but not sufficient for dispersal, since they do not specify how efficiently momentum and energy are transferred in the flow-core interaction. A detailed treatment of this question requires realistic models of the circumstellar material and of the outflow mechanism—both presently uncertain.

Despite these uncertainties, comparison of the line widths of cores with and without CO outflow suggests that the flow-core interaction is frequently strong enough to substantially increase the nonthermal part of the NH_3 line width. Figure 7 illustrates this point for 12 cores having CO outflow, listed in Table 5, and for 31 cores within the same range of distance (500 pc) known not to have outflow from the surveys of Goldsmith *et al.* (1984; one core) and this paper (seven cores); or presumed not to have an outflow because they have no embedded star according to near-infrared and *IRAS* searches (Beichman *et al.* 1986; 23 cores). Figure 7 shows that the cores with CO outflow have substantially broader nonthermal line widths than those without CO outflow: the typical ratio of nonthermal line widths probably lies in the range 1.4 (ratio of medians) to 2.1 (ratio of means). The excess in mean momentum (i.e., $M\sigma$) of cores with outflow over the mean momentum of cores without outflow is then $\sim 0.1\ M_\odot$ km s^{-1}, assuming a constant 1 $M_\odot$ core, essentially the same as the mean momentum of cores without outflow. Similarly, the excess in mean kinetic energy, i.e., $M\sigma^2$, of cores with outflow over that of cores without outflow is 8×10^{41} ergs, ~ 4 times greater than the mean kinetic energy of cores without outflow. These

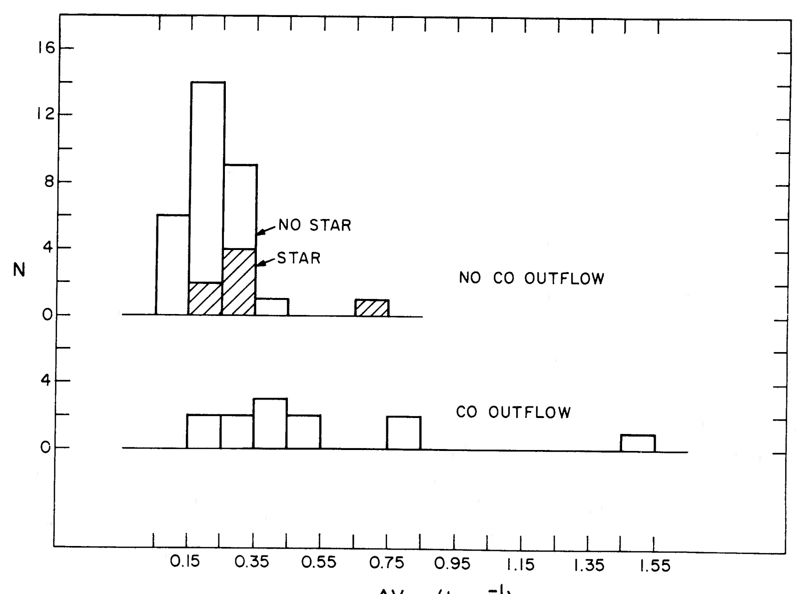

FIG. 7.—Distribution of the nonthermal part of the NH_3 line width for 12 cores with CO outflow in Table 5 and 31 cores without outflow within the same distance range. Cores without outflow but with associated stars are indicated with shading.

TABLE 5

MOMENTA OF LOW-MASS CORES AND OUTFLOWS

Core	Reference	Distance (pc)	Reference	P_{core} ($M_\odot$ km s^{-1})	P_{flow} ($M_\odot$ km s^{-1})	Reference
B5	1	350	2	0.86	0.30	3
L1455	4	350	2	4.5	4.5	5
N1333	6	350	2	20	34	7
L1489	8	140	9	0.028	0.040	10
L1551	8	140	9	0.35	5.3	11
L1535	12	140	9	0.12	0.17	13
B35	1	500	14	1.4	2.0	10
L43	8	160	15	0.13	0.12	10
L723	4	300	5	0.072	1.0	5
L778	1	250	16	0.17	0.28	10
B335	8	400	17	0.15	0.30	5
L1172	8	440	14	0.23	2.3	10

REFERENCES.—(1) Benson 1983; (2) Herbig and Jones 1983; (3) Goldsmith, Langer, and Wilson 1986; (4) Torrelles *et al.* 1986; (5) Goldsmith *et al.* 1984; (6) Ho and Barrett 1980; (7) Snell and Edwards 1981; (8) Myers and Benson 1983; (9) Elias 1978*a*; (10) this paper; (11) Schloerb and Snell 1984; (12) Ungerechts, Walmsley, and Winnewisser 1982; (13) Heyer *et al.* 1987; (14) Cohen and Kuhi 1979; (15) Elias 1978*b*; (16) Beichman *et al.* 1986; (17) Bok and McCarthy 1974.

relationships do not depend significantly on whether the total, or the nonthermal part, of the line width is considered. Therefore, the line width differences in Figure 7 are consistent with a substantial increase in core momentum and kinetic energy, arising from flow-core interaction.

The conclusion that $P_{flow} \gtrsim P_{core}$ depends critically on the use of a tracer of core properties (e.g., lines of NH_3, HC_3N, or C_3H_2) which gives core size and line width close to, or smaller than, the values reported here. Since core size and line width are generally correlated (Martin and Barrett 1978; Snell 1981; Leung, Kutner, and Mead 1982; Myers 1983) a tracer line having a larger core map size than the NH_3 line will tend to have a larger line width than does the NH_3 line, and the corresponding estimate of P_{core} can exceed that based on the NH_3 line by a significant factor. In L778 the estimates of map size, line width, and P_{core} based on the $J = 2 \rightarrow 1$ line of CS (Heyer *et al.* 1986) exceed those presented here by respective factors of ~ 1.6, ~ 2.7, and ~ 30. These differences in core map size for lines of high-density tracers such as CS and NH_3 are well-established observationally, but their origin is unclear and need further study. They may arise from greater scattering by CS than by NH_3 in the relatively low-density gas around the core (Fuller and Myers 1987).

The line width relationships in Figure 7 are statistical and thus of limited significance. More decisive indications of core dispersal should arise as more detailed core maps become available. It will be useful to examine outflow sources not centered in their cores, since such an outflow may have already dispersed some of its core. Two cores that may illustrate this effect are L1489 and L43 Mathieu *et al.* (1988), each with an outflow source on the edge of its NH_3 map.

In summary, the detection rates in § III*a* indicate that CO outflows have frequency of occurrence high enough, and duration long enough, to be the primary mechanism of core dispersal. The comparisons in Table 5 and Figure 6 suggest that the typical outflow is able to significantly increase the core momentum and energy; and the core line width statistics of this section show that cores with outflows have substantially bigger line widths than cores without outflows—consistent with the idea that the typical outflow causes a substantial increase in core momentum and kinetic energy. Taken together, these results suggest that outflows traced by CO are likely to be the main agents of core dispersal. If so, outflows play a key role in determining the main-sequence mass of a star, by limiting the supply of dense gas available for collapse.

b) *Luminosities*

Stars with outflow are thought to be among the youngest known, with ages of $\sim 1 \times 10^5$ yr or less deduced from the outflow dynamical times. Such stars should therefore be younger than their nonoutflow neighbors, and comparison of neighboring outflow and nonoutflow stars may reveal differences associated with this age difference. Levreault (1985) showed that young optically visible stars having either CO outflow or other, optical indications of mass loss, or both, tend to occupy a hotter, more luminous region of the Hertzsprung-Russell diagram than otherwise similar stars having neither CO nor optical indications of mass loss. Here we make a similar comparison based on the bolometric luminosity of young stars searched for CO outflow by Levreault, by Edwards and Snell (1982), Calvet, Cantó, and Rodríguez (1983), Schloerb and Snell (1984), Goldsmith *et al.* (1984), Goldsmith, Langer, and Wilson (1986), by Heyer *et al.* (1987), and by this paper. To minimize differential sensitivity arising from a large range in distance we consider only stars in the distance range 140–400 pc. In this range, 70 stars were searched for CO outflow, and outflows were detected and mapped in 17. The luminosities were combined from estimates by Cohen and Kuhi (1979) for optically visible stars; from Elias (1978*a*, *b*) and Myers *et al.* (1987) for stars with significant near-infrared emission; and from Beichman *et al.* (1984, 1986) for *IRAS* sources. A bolometric correction was applied as described by Myers *et al.* (1987). Most of these stars are in Taurus-Auriga, where the *IRAS* sensitivity limit on luminosity is $\sim 0.1\ L_\odot$.

Figure 8 shows the number distribution of bolometric luminosity for stars with and without CO outflow. A significant shift is evident in the distributions: 17 stars with CO outflow have luminosity $12 \pm 6\ L_\odot$ (mean $\pm$ standard error of the mean) while 53 stars without CO outflow have $4 \pm 2\ L_\odot$. If the highest luminosity is dropped from each sample, the stars with CO outflow have $7 \pm 2\ L_\odot$ and those without outflow have $2.4 \pm 0.6\ L_\odot$. In either case, the ratio of mean luminosities is $\sim 2.9 \pm 0.3$. Another description of the distributions is the median luminosities, 5.2 and 1.2 $L_\odot$, with a ratio of 4.

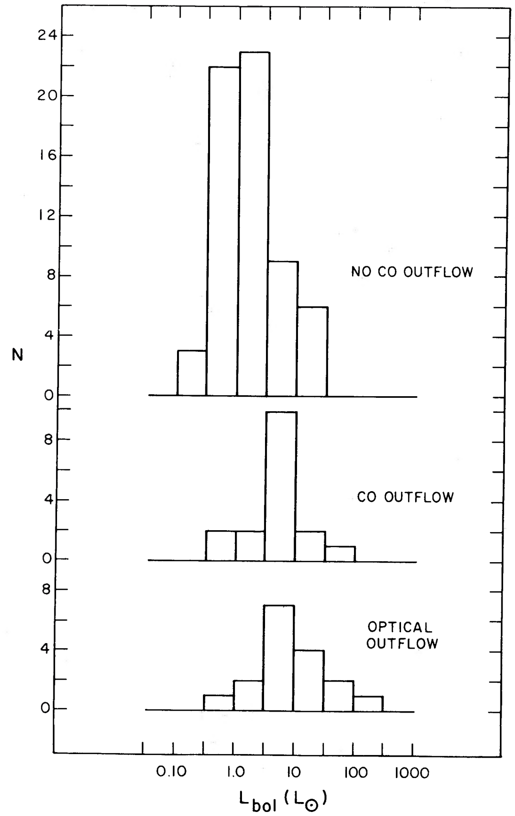

FIG. 8.—Distributions of bolometric luminosity for stars within 400 pc. *Upper plot:* 53 stars without CO outflow. *Middle plot:* 17 stars with CO outflow. *Lower plot:* 17 stars with optical indications of outflow.

Thus, within 400 pc the typical star with CO outflow has luminosity greater than that of the typical star without CO outflow by a factor of 3–4.

Figure 8 also shows the distribution of luminosity of 17 stars within 400 pc having optical indications of mass loss— optical jet, cometary nebulosity, Herbig-Haro objects, or P Cygni profile in the Hα line—according to Mundt *et al.* (1985) and Strom *et al.* (1986). Their luminosity distribution is similar to that of the objects with CO outflow, although the two groups have only four stars in common. Thus, within 400 pc, stars with CO or optical indications of mass loss, or both, have typical luminosity 3–4 times greater than neighboring young stars without such mass loss.

The simplest interpretation of this situation is that outflows are easier to detect from stars with high luminosity than from stars with low luminosity. For reasons not entirely clear, CO outflow luminosity is roughly correlated with stellar luminosity (Bally and Lada 1983). When the low-luminosity sources discussed in this paper are combined with those of Bally and Lada, this correlation becomes more significant. Therefore, it is possible that young low-luminosity stars have weak CO outflow that escaped detection in previous surveys. Alternatively, the typical star with outflow may be younger than the typical star without outflow, and thus more luminous. A more sensitive CO survey may reveal whether the apparent shift in the histograms in Figure 8 is real or due to sensitivity limitations.

IV. SUMMARY

The main points presented in this paper are as follows.

1. Twenty-six dense cores in dark clouds were surveyed for outflow in the J = 1–0 line of ^{12}CO at 2.6 mm. Sixteen of these have an *IRAS* source within one NH_3 map diameter of the map peak. Of these 16 cores with stars, seven have CO outflow. Of the remaining 10 cores, none has an outflow.

2. The detected outflows are among the weakest known, with mass loss rates of $\sim 10^{-8}\ M_\odot\ \mathrm{yr}^{-1}$ or less, comparable to the mass loss rates of winds from T Tauri stars.

3. In contrast to most CO outflows, those presented here have nearly equal ^{12}CO and ^{13}CO line intensity at the velocity of peak ^{13}CO emission, suggesting relatively large column densities of CO gas. This property may be a useful indicator of the presence of a core.

4. The high fraction of outflows detected from cores with stars, 0.4, may imply a value higher than 0.5–0.7 when account is taken of previously discovered outflows from cores with stars, of the bias against detecting outflows whose axes are perpendicular to the line of sight, and of outflows with size smaller than the resolution of this survey.

5. The high fraction of outflows in cores with stars implies that most such cores have CO outflow at some time during the life of the star-core system and that the typical outflow lasts for most of the life of the star-core system.

6. For 12 outflows from dense cores in dark clouds, the outflow momentum is similar to, or greater than the product of core mass and core velocity dispersion derived from NH_3 line data. This implies that the typical outflow has enough momentum and kinetic energy to substantially increase the internal motions of the core gas and, thus, to disperse the core.

7. For 12 cores with CO outflow, the nonthermal part of the NH_3 velocity dispersion is significantly greater than that for 31 cores without CO outflow. Cores with outflow have mean velocity dispersion twice as great, and mean kinetic energy 4 times as great, as those for cores without outflow. This implies that the typical outflow couples enough of the momentum and energy to the core to significantly increase the motions of the core gas. Together with points 5 and 6, this suggests that outflows traced by CO are the main agent of core dispersal. If so, outflows help determine the main-sequence mass of low-mass stars by removing dense gas available for accretion.

8. Bolometric luminosities were compiled for 70 stars within 400 pc, of which 17 have CO outflow. The stars with CO outflow are typically 3–4 times more luminous than those without CO outflow. Seventeen stars within 400 pc having optical indications of outflow have a luminosity distribution similar to that for stars with CO outflow. Outflow surveys of low-luminosity stars should reveal whether these effects are due to sensitivity limitations or differences in evolutionary state.

We thank the administrative and technical staffs of the Five College Radio Astronomy Observatory for support and assistance; and R. Levreault, S. Strom, and K. Strom for helpful discussions. The Five College Radio Astronomy Observatory is operated with support from the National Science Foundation and with the permission of the Metropolitan District Commission.

REFERENCES

Bally, J., and Lada, C. 1983, *Ap. J.*, **265**, 824.
Beichman, C., Myers, P., Emerson, J., Harris, S., Mathieu, R., Benson, P., and Jennings, R. 1986, *Ap. J.*, **307**, 337.
Benson, P. 1983, unpublished Ph.D. thesis, Massachusetts Institute of Technology, Department of Physics.
Benson, P., Goodman, A., and Myers, P. 1988, in preparation.
Benson, P., and Myers, P. 1983, *Ap. J.*, **270**, 589.
Benson, P. J., Myers, P. C., and Wright, E. L. 1984, *Ap. J.* (*Letters*), **279**, L27.
Bok, B., and McCarthy, C. 1974, *A.J.*, **79**, 42.
Calvet, N., Cantó, J., and Rodriguez, L. 1983, *Ap. J.*, **268**, 739.
Cernicharo, J., Guélin, M., and Askne, J. 1984, *Astr. Ap.*, **138**, 371.
Choe, S. 1985, *J. Korean E. S. E. S.*, **6**, 41.
Churchwell, E., Winnewisser, G., and Walmsley, M. 1978, *Astr. Ap.*, **139**.
Cohen, M. 1980, *A.J.*, **85**, 29.
Cohen, M., and Kuhi, L. 1979, *Ap. J. Suppl.*, **41**, 743.
Edwards, S., and Snell, R. 1982, *Ap. J.*, **261**, 151.
———. 1983, *Ap. J.*, **270**, 605.
———. 1984, *Ap. J.*, **281**, 237.
Elias, J. 1978*a*, *Ap. J.*, **223**, 859.
———. 1978*b*, *Ap. J.*, **224**, 857.
Elmegreen, D., and Elmegreen, B. 1978, *Ap. J.*, **220**, 51.
Frerking, M., and Langer, W. 1982, *Ap. J.*, **256**, 523.
Fuller, G., and Myers, P. 1987, in *NATO/ASI Physical Processes in Interstellar Clouds*, ed. G. Morfill and M. Scholer (Dordrecht: Reidel), p. 137.
Gaida, M., Ungerechts, H., and Winnewisser, G. 1984, *Astr. Ap.*, **137**, 17.
Goldsmith, P., Langer, W., and Wilson, R. 1986, *Ap. J.* (*Letters*), **303**, L11.
Goldsmith, P., Snell, R., Hemeon-Heyer, M., and Langer W. 1984, *Ap. J.*, **286**, 599.
Herbig, G., and Jones, B. 1983, *A.J.*, **88**, 1040.
Herbst, W., and Warner, J. 1981, *A.J.*, **86**, 885.
Heyer, M., Snell, R., Goldsmith, P., and Myers, P. 1987, *Ap. J.*, **321**, 370.
Heyer, M., Snell, R., Goldsmith, P., Strom, S., and Strom, K. 1986, *Ap. J.*, **308**, 134.
Ho, P., and Barratt, A. 1980, *Ap. J.*, **237**, 38.
IRAS Point Source Catalog. 1985, Joint IRAS Science Working Group (Washington, DC: US Government Printing Office).
Lada, C. 1985, in *Ann. Rev. Astr. Ap.*, **23**, ed. G. Burbidge, D. Layzer, and J.Phillips (Palo Alto: Annual Reviews, Inc.), p. 267.
Lada, C., and Black, J. 1976, *Ap. J.* (*Letters*), **203**, L75.
Lada, C., Thronson, H., Smith, H., Harper, D., Keene, J., Loewenstein, R., and Smith, J. 1981, *Ap. J.* (*Letters*), **251**, L91.
Leung, C., Kutner, M., and Mead, K. 1982, *Ap. J.*, **262**, 583.
Levreault, R. L. 1983. *Ap. J.*, **265**, 855.
———. 1985, unpublished Ph.D. thesis, University of Texas at Austin, Department of Astronomy.
Little, L., MacDonald, G., Riley, P., and Matheson, D. 1979, *M.N.R.A.S.*, **189**, 539.
Martin, R. N. and Barrett, A. H. 1978, *Ap. J. Suppl.*, **36**, 1.
Mathieu, R. D., Benson, P. J., Fuller, G. A., Myers, P. C., and Schild, R. E. 1988, *Ap. J.*, submitted.
Mendoza, E. 1958, *Ap. J.*, **128**, 207.
Mundt, R., Stocke, J., Strom, S., Strom, K., and Anderson, E. 1985, *Ap. J.* (*Letters*), **297**, L41.
Myers, P. 1983, *Ap. J.*, **270**, 105.
Myers, P., and Benson, P. 1983, *Ap. J.*, **266**, 309.
Myers, P., Fuller, G., Mathieu, R., Beichman, C., Benson, P. J., Schild, R., and Emerson, J. 1987, *Ap. J.*, **319**, 340.
Myers, P. C., Linke, R. A., and Benson, P. J. 1983, *Ap. J.*, **264**, 517.
Schloerb, P., and Snell, R. 1984, *Ap. J.*, **283**, 129.
Snell, R. 1981, *Ap. J. Suppl.*, **45**, 121.
Snell, R., and Edwards, S. 1981, *Ap. J.*, **251**, 103.
Snell, R., Loren, R., and Plambeck, R. 1980, *Ap. J.* (*Letters*), **239**, L17.
Strom, K., Strom, S., Wolff, S., Morgan, J., and Wenz, M. 1986, *Ap. J. Suppl.*, **62**, 39.
Terebey, S., Vogel, S. N., and Myers, P. C. 1988, in *Galactic and Extragalactic Star Formation*, ed. R. E. Pudritz and M. Fich (Dordrecht: Reidel), in press.
Torrelles, J., Ho, P., Moran, J., Rodriguez, L., and Cantó, J. 1986, *Ap. J.*, **307**, 787.
Ungerechts, H., Walmsley, M., and Winnewisser, G. 1982, *Astr. Ap.*, **111**, 339.

PAUL GOLDSMITH and RONALD SNELL: Five College Radio Astronomy Observatory, University of Massachusetts, Amherst, MA 01002

MARK HEYER: Carnegie Institution of Washington, Department of Terrestrial Magnetism, 5241 Broad Branch Road, N.W., Washington, DC 20015

PHILIP MYERS: Harvard-Smithsonian Center for Astrophysics, 60 Garden Street, Cambridge, MA 02138